Numerical Solutions for Swinging Atwood's Machine

Étienne Cadotte, Irina Nitu

December 5, 2023

1 Introduction

In 1784, English mathematician George Atwood implemented an experiment to verify the laws of motion. It consists of two masses connected by a mass-less string passing over a pulley, with each mass dangling on one side of the pulley. Under the influence of gravitational acceleration, the heavier mass slides down, pulling the smaller mass up along the vertical axis. While such a problem is quite simple to analyze and is often used in high school, its simplicity is based on an assumption that the motion of the masses is locked about the vertical axis, thus neglecting the angular motion of the masses. In this paper, we will analyze the much more complex problem involving one or both masses free to swing. We will make use of various integrators to numerically resolve the mass trajectories for various sets of values, and analyze the numerical precision of our simulations, namely with respect to conservation of energy.

2 The Equations of Motion

Before doing any numerical work on the system, we need to find the equation of motions of the system. Here, we will derive them through Hamiltonian dynamics. Assuming a mass-less string and small pulley, we can write the kinetic energy as :

$$T = \frac{1}{2}M\dot{r}^2 + \frac{1}{2} * m * (\dot{r}^2 + r^2\dot{\theta}^2),$$

which comes from $T = \frac{1}{2}mv^2 + \frac{1}{2}I\omega^2$. We assume that the mass M is the larger one and mass m is the only swinging mass.

Since the only potential field in the problem is gravitational, we can define the potential energy with zero point $r = 0$ thus leading to

$$U = -Mg(R - r) - mgr\cos\theta = -MgR + Mgr - mgr\cos\theta,$$

Where R is the total length of the rope. Since $-MgR$ is a constant in the potential, we can remove it without any impact on the dynamics of the system, which gives us the following equation:

$$U = Mgr - mgr\cos\theta.$$

This leaves us with the Lagrangian :

$$L = T - U = \frac{1}{2}M\dot{r}^2 + \frac{1}{2} * m * (\dot{r}^2 + r^2\dot{\theta}^2) - Mgr + mgr\cos\theta,$$

which means:

$$p_r = \frac{\partial L}{\partial \dot{r}} = (M + m)\dot{r} \quad \text{and} \quad p_\theta = \frac{\partial L}{\partial \dot{\theta}} = mr^2\dot{\theta}$$

$$\dot{r} = \frac{p_r}{M + m} \quad \text{and} \quad \dot{\theta} = \frac{p_\theta}{mr^2}.$$

We are now able to formulate the Hamiltonian as :

$$H = T + U$$

$$H = \frac{p_r^2}{2(M+m)} + \frac{p_\theta^2}{2mr^2} + Mgr - mgr\cos\theta \tag{1}$$

Which we then use to find the derivatives of momentum:

$$\dot{p_r} = -\frac{\partial H}{\partial r} = \frac{p_\theta^2}{mr^3} - Mg + mg\cos\theta \quad \text{and} \quad \dot{p_\theta} = -\frac{\partial H}{\partial \theta} = -mgr\sin\theta.$$

We then obtain the following equations of motion:

$$\begin{cases} \dot{r} = \frac{p_r}{M+m} \\ \dot{\theta} = \frac{p_\theta}{mr^2} \\ \dot{p_r} = \frac{p_\theta^2}{mr^3} - Mg + mg\cos\theta \\ \dot{p_\theta} = -mgr\sin\theta \end{cases} \tag{2}$$

which matches with the equation of motion from the literature[1].

While these derivations consider the case of a single swinging mass, we will also use results from the two swinging mass case which resolves to the following Hamiltonian:

$$H = \frac{p_r^2}{2(M+m)} + \frac{p_{\theta_M}^2}{2M(R-r)^2} + \frac{p_{\theta_m}^2}{2mr^2} - Mg(R-r)\cos\theta_M - mgr\cos\theta_m, \tag{3}$$

with corresponding equations of motion:

$$\begin{cases} \dot{r} = \frac{p_r}{M+m} \\ \dot{\theta}_M = \frac{p_{\theta_M}}{M(R-r)^2} \\ \dot{\theta}_m = \frac{p_{\theta_m}}{mr^2} \\ \dot{p_r} = -\frac{p_{\theta_M}^2}{M(R-r)^3} + \frac{p_{\theta_m}^2}{mr^3} - Mg\cos\theta_M + mg\cos\theta_m \\ \dot{p}_{\theta_M} = -Mg(R-r)\sin\theta_M \\ \dot{p}_{\theta_m} = -mgr\sin\theta_m \end{cases} \tag{4}$$

The equations of motion we have just derived above for the single swinging mass (eq. 2), as well as for system with two swinging masses (eq. 4) will serve as our basis in our numerical resolution of mass motion.

[1]Nick Tufillaro; Integrable motion of a swinging Atwood's machine. Am. J. Phys. 1 February 1986; 54 (2): 142–143. https://doi.org/10.1119/1.14710

3 Independence Under Mass Multiplication

The first thing to be noted, as it will impact the rest of this paper, is that the dynamics of the system do not change for different masses corresponding to the same mass ratio μ; as we can see from Figure 1, the motion stays the same. With numerical analysis we find they are similar in numerical precision, thus proving that the system is only dependent on mass ratio μ, which can also be shown analytically. The method used to produce this figure will be explained in the next section. We can thus set mass $m = 1$ without any loss of generality. This lets us simplify the Hamiltonian (1) and the equations of motion(2) for the system with one swinging mass to have m=1 and M=μ.

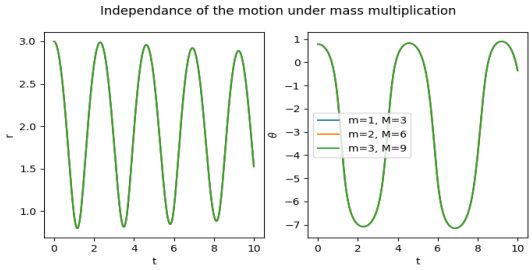

Figure 1: Paths for different masses with same mass ratio μ.

4 Our Integrators

Numerical solutions to the swinging atwood's machine were implemented with the use of an RK4 integrator which involves computing the coordinates of the system in time with four steps. We generalize the equations of motion from 2 to the following form:

$$\frac{dy(t)}{dt} = f(y(t), t). \tag{5}$$

The steps involved in the RK4 update are then

$$\begin{aligned} k_1 &= f(t_0, y(t_0)) \\ k_2 &= f(t_0 + \frac{\Delta t}{2}, y(t_0) + k_1 \frac{\Delta t}{2}) \\ k_3 &= f(y(t_0) + k_2 \frac{\Delta t}{2}, t_0 + \frac{\Delta t}{2}) \\ k_4 &= f(y(t_0) + k_3 \Delta t, t_0 + \Delta t), \end{aligned}$$

for each canonical coordinate r, θ, p_r and p_θ, which gives us the following implementation:

```
import numpy as np
def RK4(nsteps, dt, x0, derivs):
    x = np.zeros((nsteps, len(x0)))
    x[0] = x0
    break_i = nsteps
    for i in range(1,nsteps):
        f = derivs((i-1)*dt, x[i-1])
        f1 = derivs((i-1)*dt + dt/2, x[i-1] + f*dt/2)
        f2 = derivs((i-1)*dt + dt/2, x[i-1] + f1*dt/2)
        f3 = derivs(i*dt, x[i-1] + f2*dt)
        x[i] = x[i-1] + dt*(f + 2*f1 + 2*f2 + f3)/6
        if x[i][0] <= 0.1 :
            break_i = i
            break
    return x, break_i
```

where x is the vector containing the canonical coordinates r, θ, p_r, p_θ of the SAM system, and the *derivs* parameter corresponds to a function implementing equations 2.

We also make use of a Leapfrog integrator which makes use of the following second derivatives of the equations of motion 2:

$$\begin{cases} \ddot{r} = \frac{\dot{p}_r}{m+M} \\ \ddot{p_r} = \frac{2p_\theta \dot{p}_\theta}{mr^3} - \frac{3p_\theta^2 \dot{r}}{mr^4} - mg\sin\theta\dot{\theta} \\ \ddot{\theta} = \frac{\dot{p}_\theta}{mr^2} - 2\frac{p_\theta \dot{r}}{mr^3} \\ \ddot{p_\theta} = -mg(\dot{r}\sin\theta + r\cos\theta\dot{\theta}), \end{cases} \tag{6}$$

to update the system in time according to the following leapfrog update:

$$\begin{aligned} x_{n+1/2} &= x_n + \frac{1}{2}\Delta t \cdot \dot{x}_n \\ \dot{x}_{n+1} &= \dot{x}_n + \Delta t \cdot \ddot{x}_{n+1/2} \\ x_{n+1} &= x_{n+1/2} + \frac{1}{2}\Delta t \cdot \dot{x}_{n+1} \end{aligned}$$

where x represents the canonical coordinates r, θ, p_r, p_θ of the system.

The integrator is then implemented in our code as follows:

```
def leapfrog(nsteps, dt, x0, derivs2):

x = np.zeros((nsteps, len(x0)))
x[0] = x0
break_i = nsteps

for i in range(1, nsteps):
    dx, d2x = derivs2((i-1)*dt, x[i-1])
    x12 = x[i-1] + 0.5*dt*dx
    dx_12, d2x_12 = derivs2((i+0.5)*dt, x12)
    dx_new = dx + dt*d2x_12
    x[i] = x12 + 0.5*dt*dx_new

    if x[i][0] <= 0.1 :
        break_i = i
        break

return x, break_i
```

where *derivs*2 is the function which computes the second derivatives of the equation of motion of the system:

```
import numpy as np
def derivs2(t,x):
    r,pr,theta,p_theta = x
    # compute first derivatives
    dr = pr/(M+m)
    dpr = p_theta**2 / (m*r**3) - M*scipy.constants.g + m*scipy.constants.g*np.cos(theta)
    dtheta = p_theta / (m*r**2)
    dp_theta = -m*scipy.constants.g*r*np.sin(theta)
    # compute second derivatives
    d2r = dpr/(M+m)
    d2pr = 2*p_theta*dp_theta/(m*r**3)
        -3*p_theta**2*dr/(m*r**4)-m*scipy.constants.g*np.sin(theta)*dtheta
    d2theta = dp_theta/(m*r**2)-2*p_theta*dr/(m*r**3)
    d2p_theta = -m*scipy.constants.g*(dr*np.sin(theta)+r*np.cos(theta)*dtheta)

    return np.array([dr,dpr,dtheta,dp_theta]), np.array([d2r, d2pr, d2theta, d2p_theta])
```

In the repository, we can find an animated simulation of the system for mass ratio $\mu = 3$ ($results/Anim\_u = 3 - 1S - Explicit.gif$). On the right-hand side of the animation, we show the difference from the initial energy as a percentage. As we can see, the energy is properly conserved, which is expected for the Hamiltonian of a closed system. The reason why this value of mass ratio μ has been chosen is because it is the only properly integrable case of this

system as shown by Nick Tufillaro [2]. Please note that while this is the only properly integrable case, we will not restrict ourselves to it in this paper as we are using numerical simulations.

Please also note how the trajectory followed in the animation is non-singular and quasiperiodic; in this paper, we will limit our classification to singular or not singular, and periodic, quasiperiodic or chaotic. The fact that the path in the current simulation is only quasi-periodic means that if we did use a symplectic integrator, the improvement in the conservation of the Hamiltonian would have only been marginal as these integrators are specifically used for periodic motions.

As already stated, a good measurement of the quality of our integrator is the conservation of energy. Logarithmic plots of the change in energy dE as a function of step number will vary in slope depending on the type of integrator used. To do such an analysis we use our integrator and iterate over an array of step sizes. For each step size, we compute and save the difference between the initial energy at timestep 0, and the final energy at the last timestep.

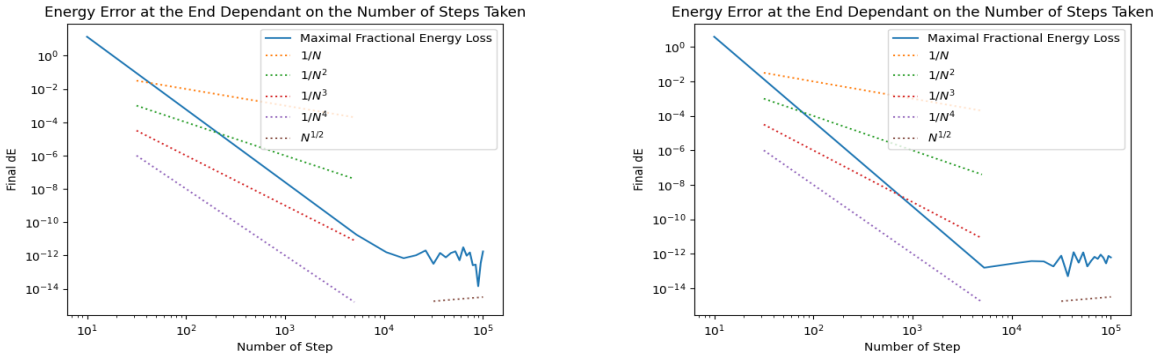

(a) Energy Error as a Function of Step Number for Quasiperiodic Motion (μ=3)

(b) Energy Error as a Function of the Number of Steps for Periodic Motion With P=π (μ=1.665)

Figure 2: Energy Errors by Step Number for the Single Swinging Mass System

This produces Figure 2a. As we can see, the base error is very large since this is a complex system but seems to follow a slope proportional to $1/N^4$, where N is the number of steps, which is similar to the performance of the leapfrog integrator in that regard, as shown in Figure 5 in appendix **??**. Overall, the number of steps required to reach what is the round-off limit of $N^{1/2}$ given by Brouwer's Law[3] is about 10^5 which is once again comparable to leapfrog.

However, as stated previously, the motion for $\mu = 3$ is only quasiperiodic. And while symplectic integrators do especially better over full periodic orbit, explicit integrators such as our own do also get some benefit. For a swinging Atwood machine, it is known from the literature that a mass ratio $\mu = 2.394$ results in a periodic path [4]. This can be visually confirmed through the animation for $\mu = 1.665$ which can once again be found in the repository ($results/Anim\_u = 1,665 - 1S - Explicit.gif$). This plot also shows the period to be about π. This acts as a perfect example of the possible periodicity against quasiperiodicity of the system.

By using μ and the period from the code above, we get Figure 2b which illustrates an improvement in the slope. Admittedly this is not by much but having a symplectic integrator would have made the improvement larger. This improvement is because in a periodic motion, over a full period where the update scheme is good, all the characteristics of the system should loop around thus giving the same state and therefore the same energy.

An important case we had to consider when doing our integrator was the case of singular paths. Singular paths are paths that either start at r=0 or end there. In this paper, we limit ourselves to the latter case. This singularity leads to division by 0 in our equations of motion which is a huge problem in both the motion and the energy of the system. To solve this problem, we simply end the simulation once the integrator reaches a specified threshold near r=0. While this means that in some cases the simulation might end early, in most cases our threshold of r = 10^{-1} was small enough to distinguish singular paths from non-singular ones.

[2]Nick Tufillaro; Integrable motion of a swinging Atwood's machine. Am. J. Phys. 1 February 1986; 54 (2): 142–143. https://doi.org/10.1119/1.14710

[3]Grazier, Kevin and Newman, William and Hyman, James and Sharp, P.W.. (2005). Long simulations of the Solar System: Brouwer's Law and Chaos. http://www.math.auckland.ac.nz/Research/Reports/view.php?id=527. 46. 10.21914/anziamj.v46i0.1008.

[4]Nicholas B. Tufillaro, Tyler A. Abbott, David J. Griffiths; Swinging Atwood's Machine. Am. J. Phys. 1 October 1984; 52 (10): 895–903. https://doi.org/10.1119/1.13791

5 Trajectories

As already stated, the paths can be divided into multiple categories. A good indicator of the performance of our integrator on non-integrable mass ratios μ is to compare the path for known quasiperiodic and non-singular μ with the path given by other integrators from literature. As we can see in Figure 3, we do indeed get quasiperiodic and non-singular paths with very small percentages in energy degeneracies for the RK4 integrator. The same thing can be said for the Leapfrog integrator, for which the trajectories of the swinging mass can be found in figure 4; although energy degeneracy percentage values are higher than the RK4 integrator, they are still relatively small. In both cases,

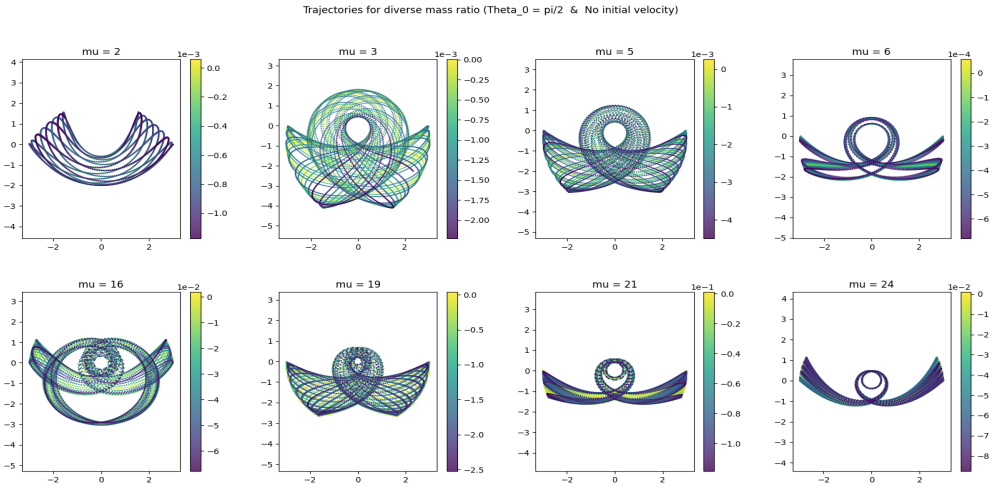

Figure 3: Quasi-Periodic trajectories colored by energy error (percentage)

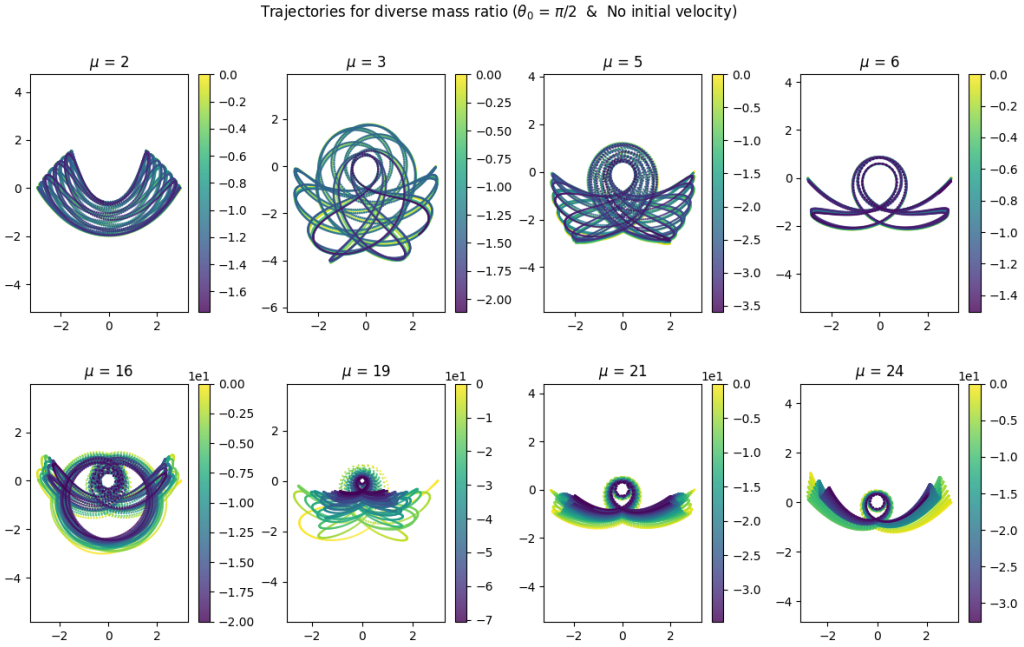

Figure 4: Leapfrog integration of the system's swinging mass m. The lighter regions indicate higher discrepencies between the inital energy of the system and the value computed at a particular point in time in the trajectory of the mass.

these curves do indeed match visually with the numerical values and theoretical from the literature[5]. Moreover, the small energy degeneracy and the consistency of our motion plots with respect to literature strongly suggest that our integrators do indeed simulate the system correctly. The difference between the energy at the last step of the simulation

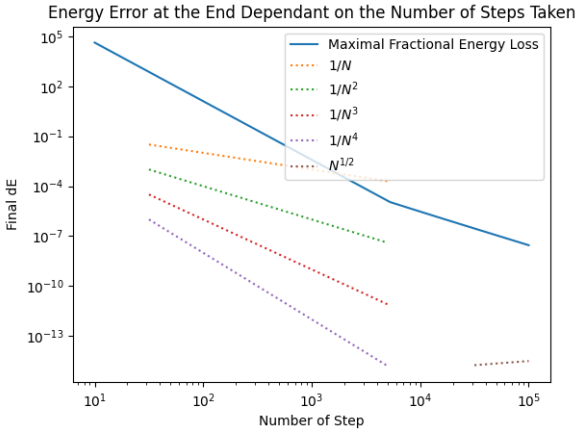

Figure 5: Leapfrog integrator energy error dE as a function of step number N.

and the first one is then computed as a function of step number N, resulting in the logarithmic plot in figure 5. It shows the error scaling proportionally with $1/N^4$ until $N = 10^4$, after which it scales with $1/N^2$, outperforming the RK4 integrator in numerical precision which scales with $N^{1/2}$ in the aforementioned region, as can be seen in figures 2b and 2a. Although the energy degeneracy fluctuates more in the Leapfrog simulations, as we can see in the trajectory plots above, the symplectic integrator performs a bit better in minimizing the energy difference between the beginning and end of the simulation.

6 Lifetime of singular orbits as an indicator of instability

We have already studied some properties of non-singular paths and have quickly touched on how we handled the singular one, but the latter case can be further analyzed to uncover some interesting properties. Such a trajectory can once again be viewed in the repository with $\mu = 10$ ($results/Anim\_\mu = 10 - 1S - Explicit.gif$).

One really interesting property of such motions is their lifetime. How does the lifetime of singular paths evolve with respect to the mass ratio μ?

The result is displayed in Figure 6 which includes the maximal energy error over the duration of integration.
First, notice that the lifetime can be split into two categories: the mass ratio values μ which reach the final time, and those that do not. The first category forms the t=5 line and can be mapped to the non-singular motions while the second is composed of the dips and the t=0 line which correspond to singular motions.
By comparing with the other results of this report, this binary categorization does line up with all examples used for non-singular motions, thus proving consistency. One thing to note is that there are nearly no peaks near the top horizontal line which shows that the final time has been reached; this signifies that all of our discovered singular paths have lifetimes significantly smaller than the total integration time, thus making our binary evaluation of singular or non-singular, accurate, If we increase the final time, we do not expect to observe an increase in singular points.

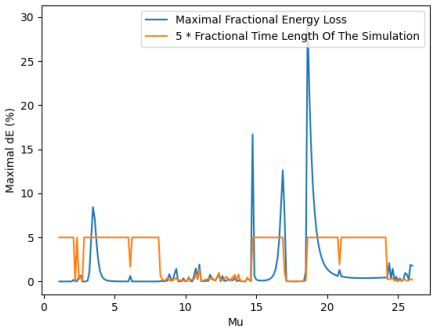

Figure 6: Energy Error and Lifetime as a Function of Mass Ratio μ

[5]Nicholas B. Tufillaro, Tyler A. Abbott, David J. Griffiths; Swinging Atwood's Machine. Am. J. Phys. 1 October 1984; 52 (10): 895–903. https://doi.org/10.1119/1.13791

The reason why we are also plotting the energy degeneracy is that it seems like there's a moderate correlation between the two. Indeed, for all singular points, we see that the energy degeneracy seems to peak at about the same points as the one where the lifetime is longer. By using numpy corrcoef after masking and normalization, we found a correlation coefficient of 0.46. This correlation is expected since being close to the singularity leads to a bigger error in energy.
We should also note that the very large peaks in energy near wells in lifetime are most likely due to the way we put a stop to simulations in which the system approaches the singularity. Since the singular paths are limited to our threshold value of r, they skip the portion near the singularity r=0 which corresponds to the region which maximizes energy error. On the other hand, the non-singular paths around it approach this region without ending the simulation, thus leading to higher peaks than in the singular case. As such, a better singularity condition could be investigated to get better results. Using more powerful computers to perform simulations with a smaller timestep dt could also be a good investigation since, according to our theory, the error should go high in the well as the points near the singularity are now being resolved for those singular motion coming in with high velocity.

7 The two mass swinging case

First, we should preface by stating that this case is a lot more of a challenge. Indeed, no literature could be found about this specific system which makes it difficult to verify the correctness of our integrator.
The system of two swinging masses extends the case with the single swinging mass by allowing the largest, second mass M, to also have angular momentum. For this system, we couldn't find any properly integrable μ to use as an analytical case. To integrate this system, we modified our integrator by applying the changing the derivative and energy equation to match Equation 4 and Equation 3

The result of our new integrator can be seen in the repository ($results/Anim\_\mu = 3 - 2S - Explicit.gif$). As we can see, the energy error stays relatively low for a mass ratio value of $\mu = 3$.

Note that if we put the initial angle of mass M to be 0, we retrieve the case with one swinging mass as expected which is good news.

We can once again plot the energy error after the entire integration time as a function of step number to compare with the known RK4 results. In doing so, we get Figure 7 where the slopes and initial values are both near identical to the single swinging, quasiperiodic case, which we already confirmed to be correct. As such, these results are just what we expect and we can say with confidence that, at least in the case where $\mu = 3$ which is used here, the energy of the distance is properly conserved given a large enough number of steps. Please note that we can only compare for what seems to be quasiperiodic over our time interval in this case as there are no known periodic μ to use when both masses are swinging.

We might as well create a plot of the trajectories of the mass m and M for the different μ we considered in Figure 3 so we can see the difference made by M having non-zero angular speed. By re-utilizing the same code with slight modifications, we can get Figure 8 for the mass m and Figure 9 for mass M.

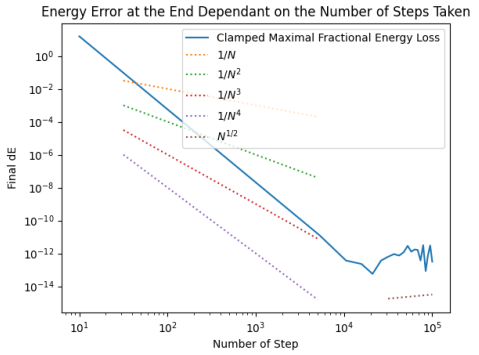

Figure 7: Energy Error by Number of Steps (μ=3)

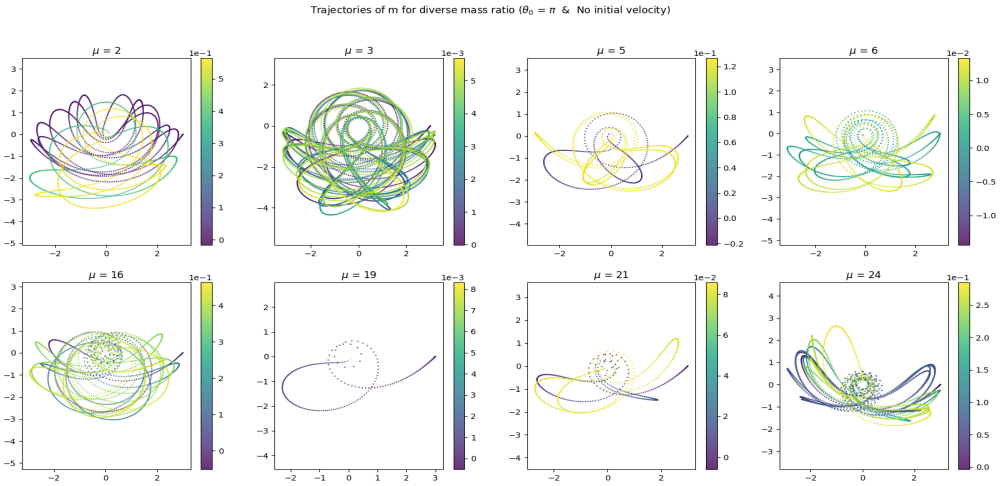

Figure 8: Trajectories colored by energy error of small mass m

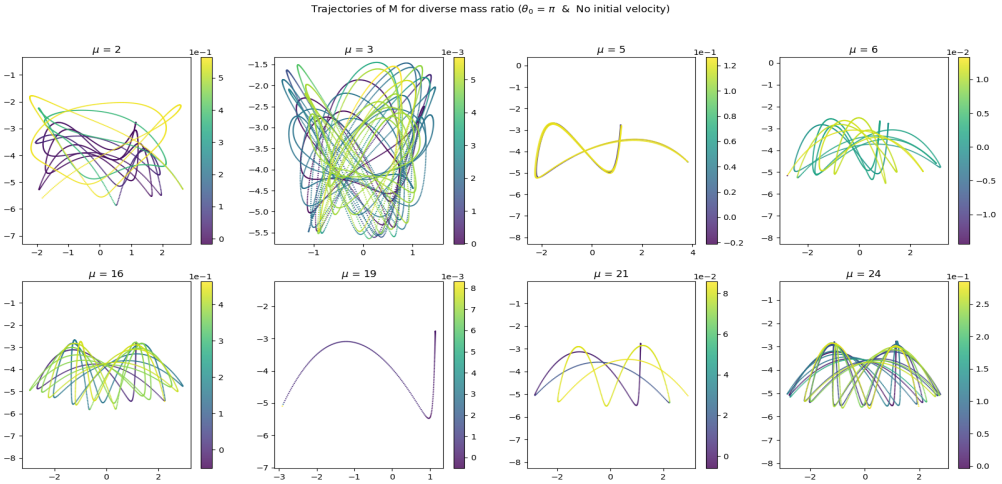

Figure 9: Trajectories colored by energy error of big mass M

An important takeaway of these trajectories is that they are not all quasiperiodic and non-singular like the one in Figure 3.
As previously stated, the mass ratio $\mu = 3$ is still quasiperiodic with respect to the trajectory of the smaller mass m but this is not the case for mass M. Furthermore, we can see in the trajectories of mass M a somewhat repeating pattern for $\mu = 16$ and $\mu = 24$. Overall, the only real conclusions we can take away from these figures are that the energy error seems to be consistently small for different mass ratios μ, and that the number of singular μ seems higher out of this small sample. We will elaborate on these two points in the following section.

To prove both of the above assumptions we will reproduce the plots from Figure 6 for the current system of two swinging masses. By doing so we get figures 10a and 10a for integration times of 100s and 1000s respectively. What we see here is very important because the plots in Figure 8 and Figure 9 were done with an integration time of 10s instead. The first noticeable thing in both plots is that our previous conclusions are both still true; the error is on average smaller than Figure 6 and we also see a lot more singular motions.
However, regarding singular motion, we see by comparing the 100s case with the 1000s one that the cases that were assumed to be quasiperiodic in the 10s are proven to be singular when increasing the final time which is contrary to what we concluded in Figure 6; this is significant as it suggests that simulations for any mass ratio values μ leads to

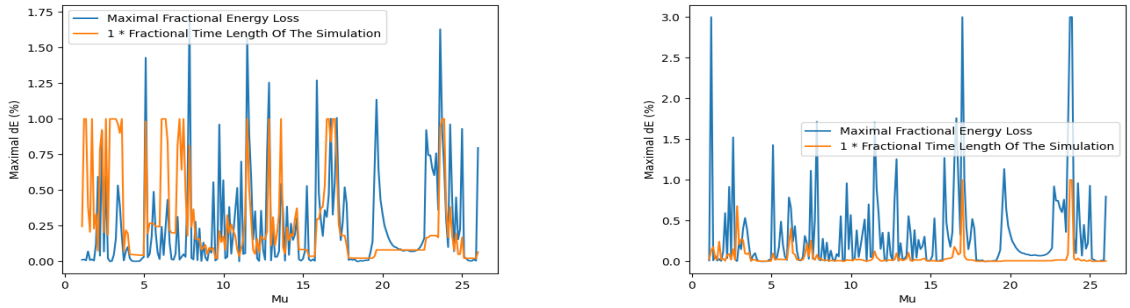

(a) Energy Error and Lifetime by μ with 2 swinging masses. $t_f = 100s$

(b) Energy Error and Lifetime by μ with 2 swinging masses. $t_f = 1000s$

Figure 10: Energy Errors and Lifetime by μ

singular motion. As such, we can say with confidence that the motion we assumed to be quasiperiodic and non-singular for $\mu = 3$ in our analysis from Figure 7 was based on a wrong assumption, as an increase in integration time reveals the motion to be singular like all the other μ.

One last thing can be pulled out of these graphs. We determined earlier that for the one swinging mass system, the energy error and the lifetime seemed to be correlated, with lower lifetimes (singularities) resulting in higher error in energy. We cannot, with certainty, conclude the same in this case, as there are next to no plateaus to analyze in our data from figure 10. We do, however, seem to see some correlation between the sparse peaks in lifetime and peaks in error which could be explained in the same manner as before, for the edges of the plateau of the Figure6. Overall, analysis of the system with two swinging masses does not lead to any definitive conclusions.

8 Future Improvement and Conclusion

In this paper, we numerically simulated the motion of the SAM for two variations, with the first consisting of one swinging mass, and the second of both masses swinging. For the former case, we implemented RK4 and Leapfrog integrators to obtain trajectory plots of the single swinging mass, and both methods were found to be in agreement with previously simulated results[6]. We then analyzed the error in energy as a function of step number N for each integrator, which was found to scale with $1/N^4$ until N reached 10^4, after which the error scaled with $N^{1/2}$ and $1/N^2$ for the RK4 and Leapfrog integrators respectively. We then analyzed simulation results for different mass ratio values μ and discussed singular cases where the radius r of the swinging mass approaches zero. Our leapfrog implementation can be used in further analyses involving singular states, and could be applied to numerically simulate the system with two swinging masses. The canonical coordinates of the system and their derivatives could also be plotted overtime to and analyzed for each integrator. Another obvious improvement, as previously state, would consist in determining a better condition for ending simulations near singularity.

9 Statement of Contribution

The explicit integrator part has been mostly done by Etienne while the symplectic was mostly by Irina. The writing of this report is a joint effort.

[6]Nick Tufillaro; Integrable motion of a swinging Atwood's machine. Am. J. Phys. 1 February 1986; 54 (2): 142–143. https://doi.org/10.1119/1.14710